

Open Access :: ISSN 1847-9286

www.jESE-online.org

Original scientific paper

# Multimetodolological characterization of an optimized carbon/np TiO<sub>2</sub> electrode

Saša Mićin<sup>1\*</sup>, Nadica Ivošević DeNardis<sup>2</sup>, Sanja Martinez<sup>3</sup>, Maja Levak Zorinc<sup>2</sup>, Borislav N. Malinović<sup>4</sup> and Vedrana Špada<sup>5</sup>

<sup>1</sup>University of Banja Luka, Faculty of Security Sciences, Banja Luka, Bosnia and Herzegovina <sup>2</sup>Ruđer Bošković Institute, Zagreb, Croatia

<sup>3</sup>University of Zagreb, Faculty of Chemical Engineering and Technology, Zagreb, Croatia <sup>4</sup>University of Banja Luka, Faculty of Technology, Banja Luka, Bosnia and Herzegovina <sup>5</sup>University of Istria, Research Center METRIS, Pula, Croatia

\*Corresponding Author: E-mail: sasa.micin@fbn.unibl.org; Tel.: +387-51-333-648

Received: MMMM DD, YYYY; Revised: MMMM DD, YYYY; Published: MMMM DD, YYYY

## **Abstract**

There is a significant need to characterize biologically active compounds, like polyphenols, which play a vital role in human health protection. We have recently proposed a method for electrochemical characterization of polyphenols in natural wine using an integrated system of modified carbon electrode with nanoparticles of TiO2 and an algorithm that could be applied in winemaking. The present work describes the optimized electrochemical sensor used in the above-mentioned study. The aim of this study is to investigate the influence of specific binders and nanoparticles on the physicochemical and electrochemical properties of modified carbon electrodes. The imaging techniques (SEM-EDS, AFM) showed that the electrode material becomes denser with a higher binder content and that the  $TiO_2$  nanoparticles are almost evenly distributed despite the manual preparation of the carbon paste. The results show that the modified carbon paste with 40 vol.% paraffin oil and 8 wt.% TiO2 nanoparticles has the lowest surface roughness, anodic current and electroactive surface area, which is consistent with the reported lowest resistance, as well as the highest degree of reversibility compared to the standard reversible redox system ([Fe(CN)]<sup>3-/4-</sup>) within the electrode material. By combining several methods, an optimized composition of carbon/ $npTiO_2$  can be determined, and used for further applications.

# **Keywords**

AFM; carbon based electrode; CV; FTIR; SEM-EDS; TiO<sub>2</sub> nanoparticles

## Introduction

Amperometric sensors based on carbon paste modified with TiO<sub>2</sub> nanoparticles have found wide application in the electroanalysis of various biologically derived substances, pharmaceutical compounds, and environmental pollutants [1]. Previous studies have shown that carbon paste electrodes modified with TiO<sub>2</sub> nanoparticles are characterized by good sensitivity, selectivity, reproducibility, and repeatability, along with a low detection limit for analytes [2].

The practical application of carbon electrodes modified with TiO<sub>2</sub> particles for electroanalytical purposes significantly depends on the physicochemical and electrochemical properties of the electrode paste. Morphological and topographical characteristics of the electrode surface are classified as physicochemical features of the sensor, which have a significant influence on the properties of the electrode material [3–5].

Spatial distribution of the modifier, surface roughness of the electrode, interactions between the carbon material, binder, and nanoparticles, as well as the type of crystalline structure of TiO<sub>2</sub> nanoparticles, are among the topographical and morphological features that impact the electrochemical properties of the carbon electrode modified with TiO<sub>2</sub> nanoparticles.

A carbon electrode modified with Ru-doped TiO<sub>2</sub> nanoparticles exhibited better electrochemical characteristics compared to an unmodified electrode. AFM topographical analysis of the modified carbon electrode indicates an increase in surface roughness due to the presence of modifier particles on the electrode surface [6]. Rajawat et al. demonstrated that the presence of a modifier (coconut shell powder) affects the morphological characteristics of the electrode surface made of graphite powder and mineral oil, leading to increased roughness [7]. Research by Liu et al. highlighted the influence of the crystallographic orientation of the modifier, BiVO<sub>4</sub> nanoparticles, on the electrochemical characteristics of the modified electrode [8]. The increase in the intensity of the anodic current peak during the electrooxidation of azithromycin on an electrode modified with TiO<sub>2</sub> nanoparticles of a tetragonal (rutile) structure was attributed by Sopaj et al. to an increase in the electroactive surface area. This was a consequence of the modifier's nanoparticles, which caused increased roughness [9]. Dobrescu et al., applying fractal theory, showed that the presence of a composite modifier, ionic liquid/AuTiO<sub>2</sub>/graphene oxide, affects the surface characteristics of the electrode material. The impact on the geometric shape of the surface and the size of the active area manifested through a more pronounced anodic current peak [10].

In addition to the type and size of the carbon material, the size and content of the modifier, i.e. the nanoparticles, the type and content of the binder and the preparation method also significantly influence the morphological and topographical characteristics of the electrode surface [11–14]. In previous studies, the most commonly used binders were chemically inert and insoluble substances in the analysed solution, such as paraffin oil (PO), aliphatic and aromatic hydrocarbons, silicone oil, silicone grease, halogenated hydrocarbons, tricresyl phosphate (TCP), dioctyl phthalate (DOP), diisononyl phthalate (DINP), diphenyl ether, glycerol, castor oil, petroleum jelly, ionic liquids, and carbon-based ionic liquids. Additionally, studies have been conducted using electroactive binders, such as a mixture of 3-methylphenyl bis(4-methylphenyl) phosphate, bis(3-methylphenyl) 4-methylphenyl phosphate, and tris(3-methylphenyl) phosphate (tricresyl phosphate) (TCP) [15]. Baez et al. observed a significant influence of binder material on the electrochemical characteristics of carbon electrodes. A comparison of electrode materials prepared using mineral oil and ionic liquids derived from N-substituted octyl pyridinium bis(trifluoromethylsulfonyl)imide with various substituents showed that electrode material with ionic liquids exhibited a larger electroactive surface area. The pronounced capacitive currents

were attributed to increased surface roughness. Vatamanu et al., using molecular dynamics simulations, demonstrated the influence of electrode surface topography on the structure of the electric double layer and differential capacitance at the graphite-ionic liquid interface [3]. A comparison of carbon electrodes modified with  $TiO_2$  nanoparticles using paraffin oil, tricresyl phosphate, and a mixture of these binders revealed varying degrees of uniformity in the spatial distribution of nanoparticles on the electrode material's surface, as well as differences in the number and size of nanoparticle agglomerates. The number and size of the agglomerates were influenced by the intensity of interactions between  $TiO_2$  particles, graphite, and the binder, as well as the physicochemical properties of the binder [16].

The aim of this study is to investigate the influence of specific binders and nanoparticles on the physicochemical and electrochemical properties of carbon electrodes/np TiO<sub>2</sub>. The multimetodological approach using scanning electron microscopy with energy dispersive X-ray spectroscopy (SEM-EDS), atomic force microscopy (AFM), Fourier transform infrared spectroscopy (FTIR) and cyclic voltammetry (CV) will provide important data to determine the optimal composition of the modified carbon electrode that we used in our previous study [17].

# **Experimental**

#### Chemicals

The following materials were used to prepare the modified electrode paste: extra-pure graphite powder with a particle size <50  $\mu$ m (CAS number 7782-42-5, Merck, Germany), diethyl ether p.a. (Lachner, Czech Republic), paraffin oil (CAS number 8042-47-5, Merck, Germany), a reaction mixture of 3-methylphenyl bis(4-methylphenyl) phosphate, bis(3-methylphenyl)-4-methylphenyl phosphate and tris(3-methylphenyl) phosphate (tricresyl phosphate) (CAS number 1330-78-5, Merck, Germany) and TiO<sub>2</sub> nanoparticles. The TiO<sub>2</sub> nanoparticles, which are commercially known as AEROXIDE® TiO<sub>2</sub>P (Evonik Industries AG, Germany), have a size of 10–50 nm and are predominantly distributed between 15 and 25 nm [18]. Distilled water with a conductivity of 4  $\mu$ S-m-1 was used to prepare the solution. Potassium hexacyanoferrate(II)  $K_4$ [Fe(CN)<sub>6</sub>]×3H<sub>2</sub>O p.a. (Kemika, Croatia) and potassium chloride KCl p.a. (Kemika, Croatia) were used to prepare the working electrolyte solution for cyclic voltammetry.

## Preparation of Modified Carbon Paste

The modified carbon paste was prepared by dispersing a mixture of graphite powder (4.6 g) and TiO<sub>2</sub> nanoparticles (0.4 g) in 50 mL of diethyl ether with constant stirring and heating to 40 °C. The solvent was then evaporated. After evaporation of the diethyl ether, the graphite powder (3 g) with dispersed TiO<sub>2</sub> particles was mixed with: a) paraffin oil (PO, 1.09 mL), b) a reaction mixture of 3-methylphenyl bis(4-methylphenyl)phosphate, bis(3-methylphenyl)4-methylphenyl phosphate, and tris(3-methylphenyl)phosphate (tricresyl phosphate, TCP, 1.09 mL) and c) a mixture of paraffin oil (0.5 mL) and tricresyl phosphate (0.5 mL) (POTCP). Homogenization was performed by manual mixing in a ceramic dish according to the procedure described in the literature [19]. The prepared modified carbon paste was stored in a sealed plastic container at room temperature and used 24 hours after preparation.

# Surface characterization of the modified carbon paste

The surface characterization of the electrode was performed using SEM-EDS and AFM. An SEM instrument (Quanta 250 FEG, FEI, USA) equipped with a low vacuum secondary electron detector

(LFD) and a backscatter electron detector (BSED) was used. The chemical analysis and mapping of the chemical elements present on the surface of the tested materials was carried out using SEM-EDS (Pentafet detector, Oxford), measuring four points for each sample. The size of each analyzed spot was 5 nm on a sample surface of 3.7 mm  $\times$  3.2 mm. For sample preparation, a thin layer of the sample was applied to a sample holder, which was then positioned for imaging.

Atomic force microscopy (AFM) was performed using a Multimode scanning probe microscope equipped with a Nanoscope IIIa controller (Bruker, Billerica, USA) and a 125 µm Vertical Engagement (JV) scanner. Topographic images were acquired in contact mode with silicon nitride scanning probes (DNP, Bruker, nominal frequency 18 kHZ, spring constant 0.06 N/m). Measurements were performed in air, at room temperature and 50-60% humidity. During imaging, the applied force was kept as low as possible to avoid possible damage to the sample. The imaging rate was kept between 1 and 2 Hz per line and at a resolution of 512 x 512. All images represent the raw data, except for the two-dimensional flattening to reduce the hysteresis effect of the scanner. The images were analyzed in the NanoScopeTM software (Digital Instruments, version V614r1). Topographical images of the surfaces and images of the deflection deviations were recorded. The topographic images provide height data and are used to determine the surface roughness Ra. The roughness, Ra, is the arithmetic mean of the absolute values of the surface height deviations (z) measured relative to the central position of the plane. The roughness was determined on a homogeneous square (2 µm x 2 µm) part of the sample surface. A 3D view of the surface was also displayed with the appropriate software. The sample was prepared for AFM imaging by homogenizing the carbon paste in a ceramic dish prior to imaging. The sample was placed directly on a double-sided adhesive tape attached to a metal disk with an area of 1.76 cm<sup>2</sup>. On one side, the adhesive tape was stuck to the metal disk, while on the other side the carbon paste was applied with a metal spatula. The excess paste was removed with a spatula until a thin paste surface suitable for imaging was obtained.

# Physicochemical characterization of the electrode

The composition of the tested electrode pastes was analyzed by FTIR with a Fourier transform infrared spectrometer (IR Spirit T with ATR component, Shimadzu, Japan) in the wavelength range of 400–4000 cm-¹. The FTIR spectra of unmodified and modified carbon pastes were compared. The FTIR results were analyzed using the SpectraGryph 1.2 application software. Sample preparation involved dissolving the tested carbon pastes by adding chloroform. The dissolved samples were then transferred in liquid form to a sodium chloride plate using a dropper. Another plate was placed over the first to spread the liquid into a thin film. The prepared sample was then placed in the sample holder of the spectrometer for analysis.

## Electrochemical characterization of the working electrode

Cyclic voltammetry (CV) measurements were performed using a potentiostat/galvanostat (PAR 273A, Princeton Applied Research, USA) with a 50 cm<sup>3</sup> electrochemical cell consisting of the working electrode (modified carbon paste electrode), a reference electrode (Ag/AgCl 3.5 M), a counter electrode (platinum plate, surface area 2.4 cm<sup>2</sup>) and the working electrolyte 0.01 M  $K_4[Fe(CN)_6]\times 3H_2O$  (a standard electrolyte with a reversible single-electron reaction). A 0.1 M KCl solution was used as the supporting electrolyte.

The measurements were carried out in the voltage range from 0.0 V to 1.0 V at a scan rate of 50 mV/s. The experiments were carried out without stirring at room temperature (23  $\pm$  1 °C) with

three consecutive measurements. Cyclic voltammograms were analyzed using Powersuite 2.40 software (Informer Technologies, Inc.). All potentials are given relative to the reference electrode. The electrochemically active surface of the electrode was determined on the basis of the Randles-Sevcik equation [20]:

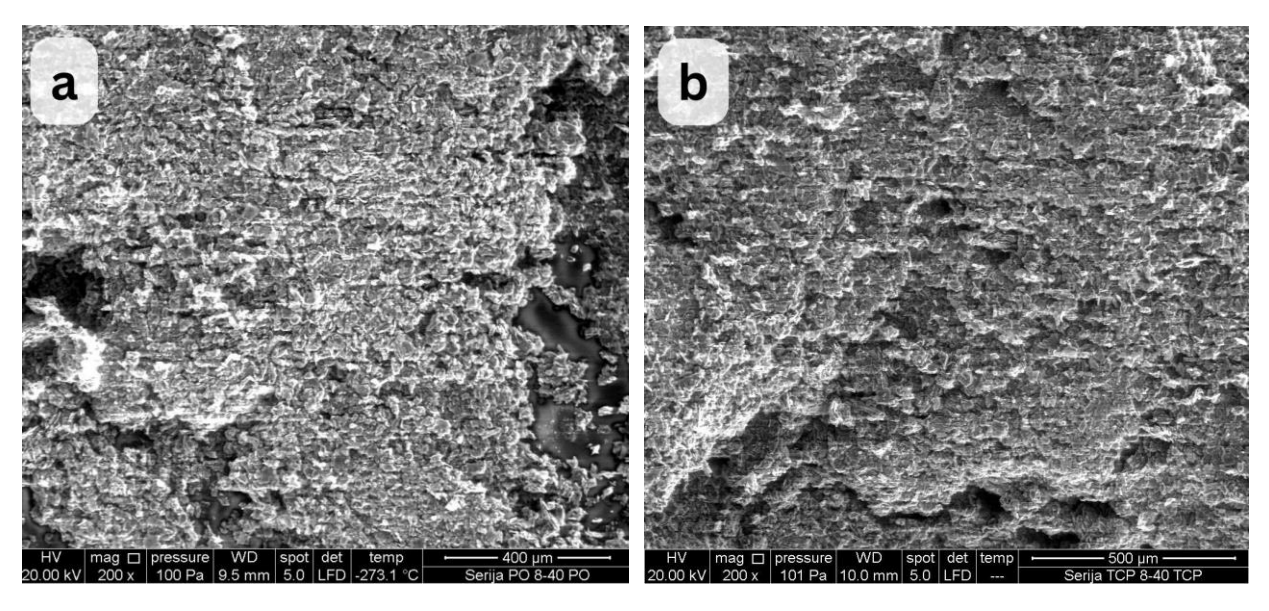
$$I_{p,a}(A) = 2,69 \times 10^5 \times z^{1/2} \times A \times D_0^{1/2} \times v^{1/2} \times c_0$$
 (1)

 $D_0$  - diffusion coefficient, v (V/s) - scan rate,  $c_0$  (mol/cm³) - concentration of electroactive species, z - number of electrons transferred, A (cm²) - electroactive surface area

#### **Results and Discussion**

Physicochemical characteristics of the modified carbon paste

The morphological characteristics of the modified carbon electrode surface were investigated using SEM. The SEM images of the surfaces of the modified carbon pastes were taken with a low vacuum secondary electron detector (LFD) at a magnification of  $200 \times (Figure 1)$ .



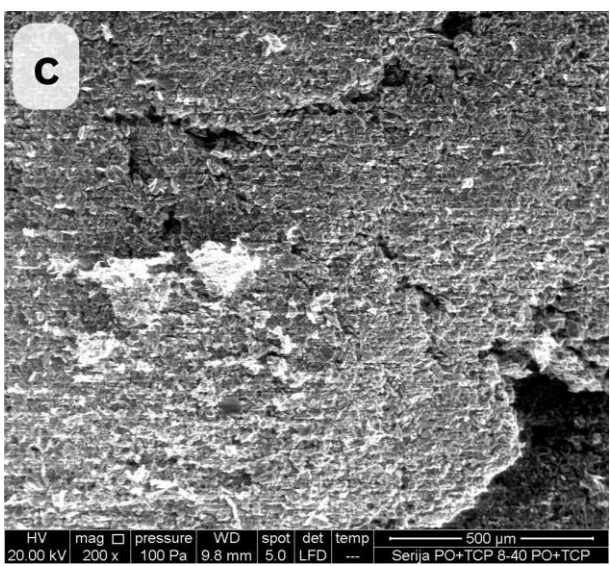


Figure 1. SEM images of the surfaces of modified carbon pastes with 8 wt.% TiO<sub>2</sub> nanoparticles and (a) 40 vol.% PO, (b) 40 vol.% TCP and (c) 40 vol.% POTCP (1:1). The images were taken in LFD mode

It can be observed that the electrode material with PO (Figure 1a) has a more pronounced geometric structure of the graphite particles than the electrode material with TCP and the POTCP (Figures 1b, 1c). Figure 2 shows SEM images of the surfaces of the modified carbon paste compositions taken with a backscattered electron detector (BSED) at a magnification of 400 ×.

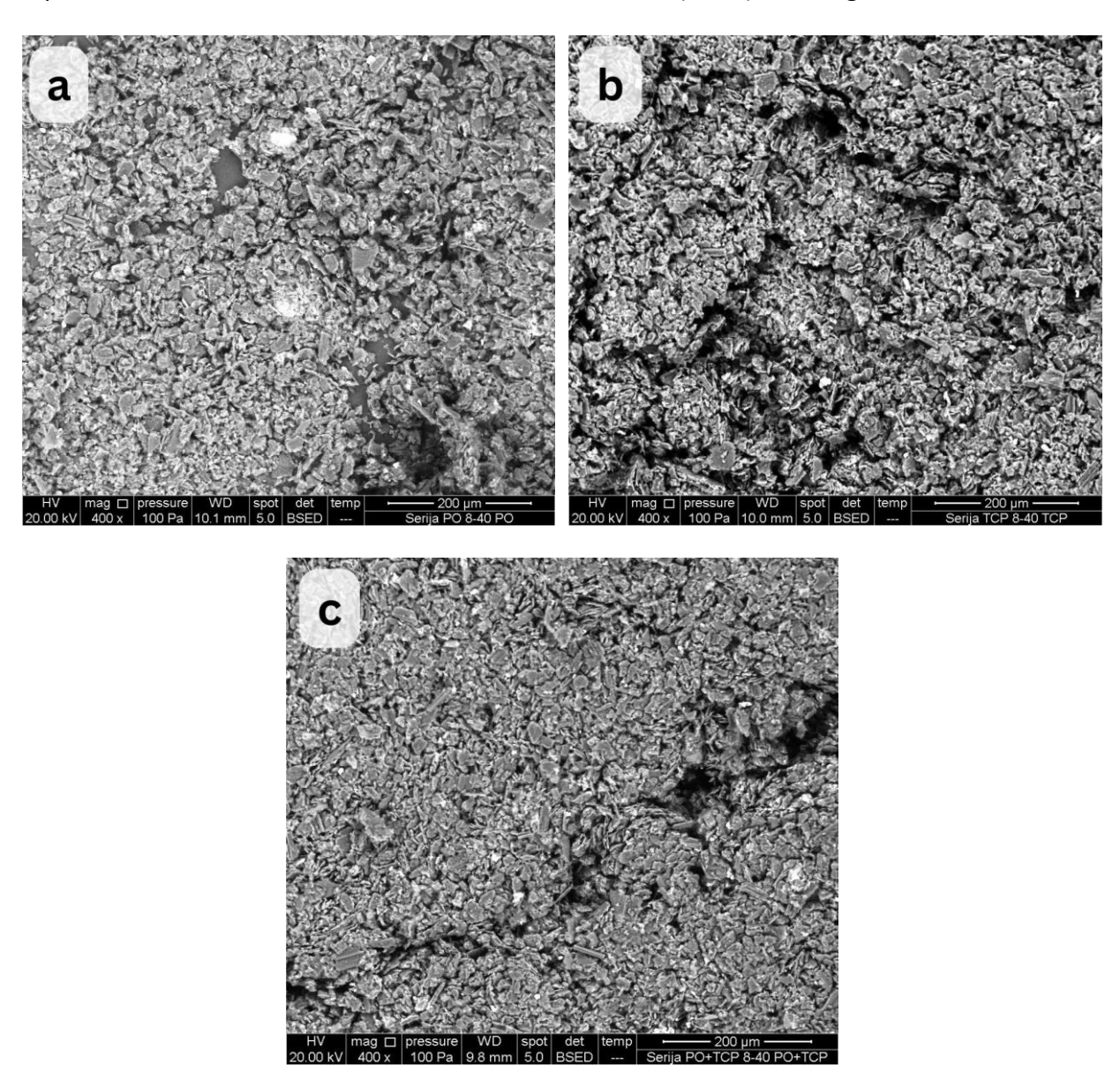


Figure 2. SEM images of the surfaces of modified carbon pastes with 8 wt.% TiO<sub>2</sub> nanoparticles and (a) 40 vol.% PO, (b) 40 vol.% TCP and (c) 40 vol.% POTCP (1:1). The images were taken in BSED mode

A comparison of the SEM images of the modified carbon pastes with PO and TCP shows that the surface with PO has a more uniform distribution of graphite particles, while the surface with TCP is characterized by a compact structure with the presence of larger graphite particle agglomerates. SEM-EDS was used to analyze the composition and elemental distribution of the electrode material. Figure 3 shows the position and ratio of the elements at the examined points of the electrode surfaces with different binders.

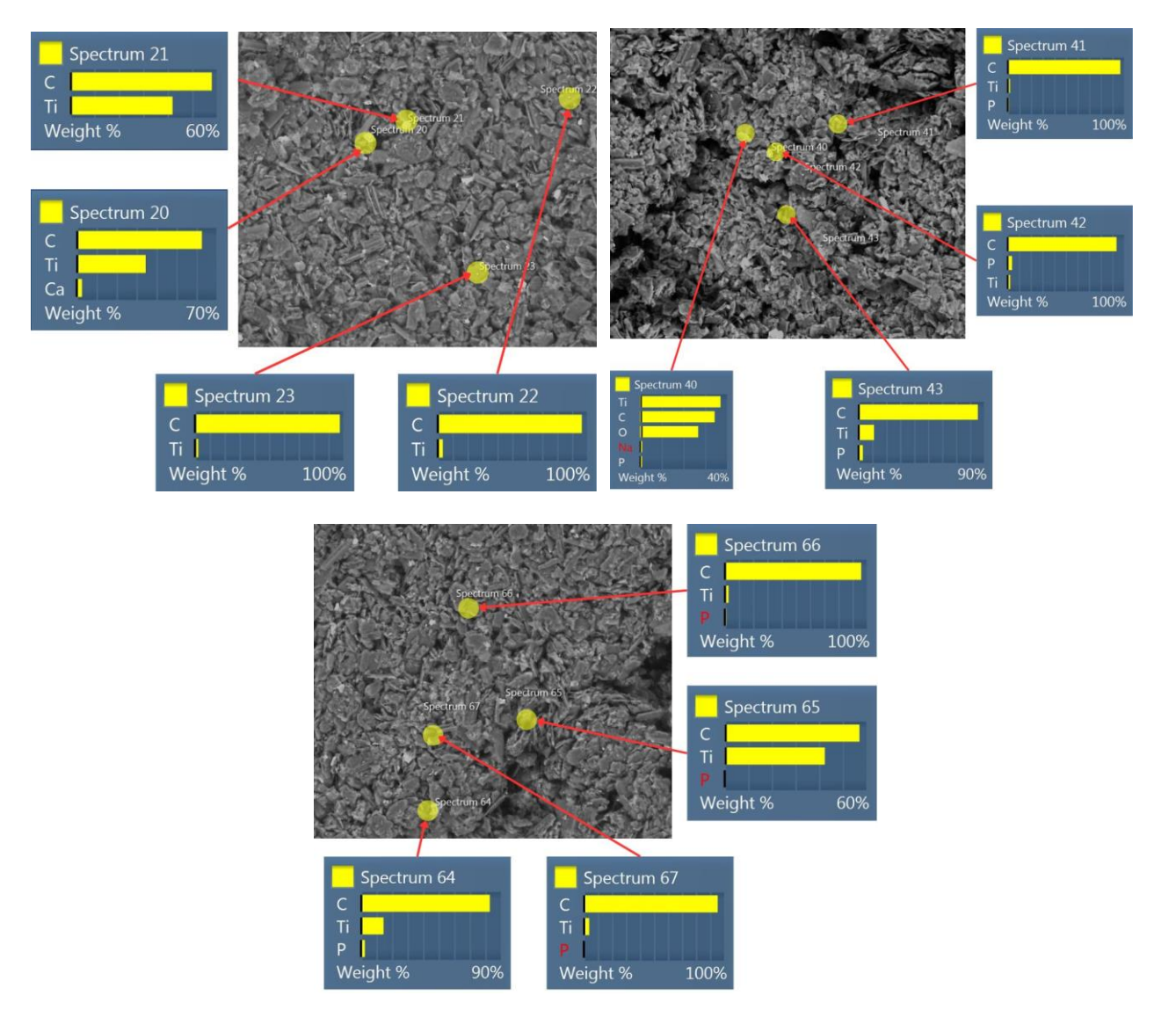


Figure 3. SEM images of the surfaces of modified carbon pastes with 8 wt.%  $TiO_2$  np and 40 vol.% PO, TCP, POTCP (1:1), with the marked positions of the analyzed points

The analysis of the chemical composition of the surface of the electrode revealed that the paste is inhomogeneous, with uneven distribution of carbon, titanium and other elements (such as iron, phosphorus or calcium), regardless of the type of binder material. The inhomogeneous chemical composition of the surface of the electrode and the presence of other atomic species (calcium, iron, oxygen) is attributed to the method of manufacturing the electrode material and traces of impurities.

The influence of the binder in the electrode material on the spatial distribution of TiO<sub>2</sub> nanoparticles on the electrode surface was analyzed by mapping the nanoparticles on the surface (Figure 4).

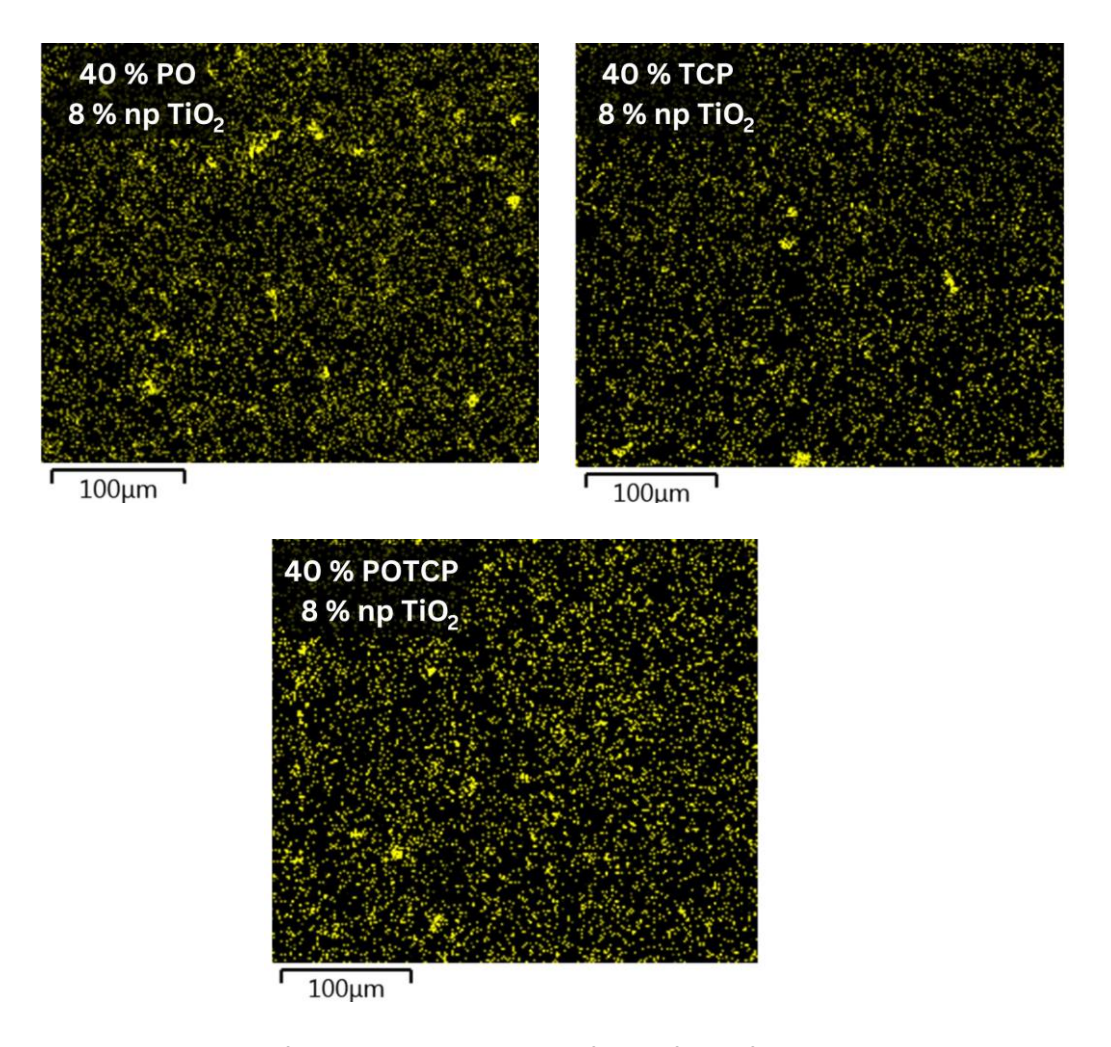


Figure 4. Spatial maps of Ti distribution on the surfaces of modified carbon pastes containing 8 wt. % TiO<sub>2</sub> np and 40 vol.% PO, TCP, POTCP (1:1)

The formation of  $TiO_2$  nanoparticle agglomerates is observed in carbon pastes with PO and TCP binders. In the paste with POTCP, the formation of a larger number of uniform agglomerates with a similar shape in a size between about 2.5  $\mu$ m and 12.5  $\mu$ m, which are relatively evenly distributed, is characteristic. It can be assumed that the number and size of the agglomerates depend on the intensity of the interactions between  $TiO_2$  particles and graphite with the binder as well as on the physical and chemical properties of the binder. In addition, the formation of agglomerated particles leads to a reduction in the active surface area of the modifier. Radoman et al. showed that added  $TiO_2$  nanoparticles dispersed in alkyd resin form agglomerates due to the large specific surface area of the modifier, which increases the intensity of the interactions between the particles [21].

The topographical features of the carbon paste electrode modified with the PO, TCP and POTCP binders and the TiO<sub>2</sub> nanoparticles were analyzed by AFM and are shown in Figure 5.

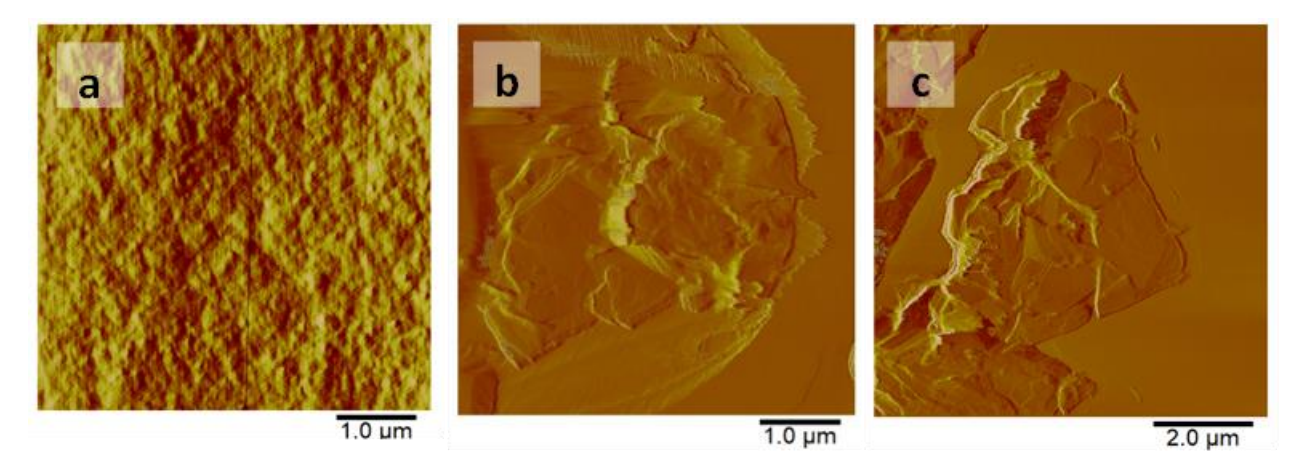


Figure 5: Deflection images of the modified carbon paste with 8 wt. %  $TiO_2$  np, and (a) 40 vol.% PO (scan size 5  $\mu$ m x 5  $\mu$ m), (b) 40 vol.% TCP (scan size 5  $\mu$ m x 5  $\mu$ m), and (c) 40 vol.% POTCP (scan size 8  $\mu$ m x 8  $\mu$ m)

The deflection images of the modified carbon paste with PO binder show a moderately granular structure on the surface (Figure 5a). The height profile (not shown) of these images shows mainly 10-40 nm deep grooves, so that the surface can be regarded as almost planar. The surface roughness determined on the modified carbon paste with PO binder is 38 nm, for TCP binder 130 nm and for POTCP binder 116 nm. For the binders TCP and POTCP (Figures 5b and 5c), however, the surface structure shown is not planar, but consists of large graphite particles or agglomerates. These particles appear to be less well bonded to the rest of the matrix.

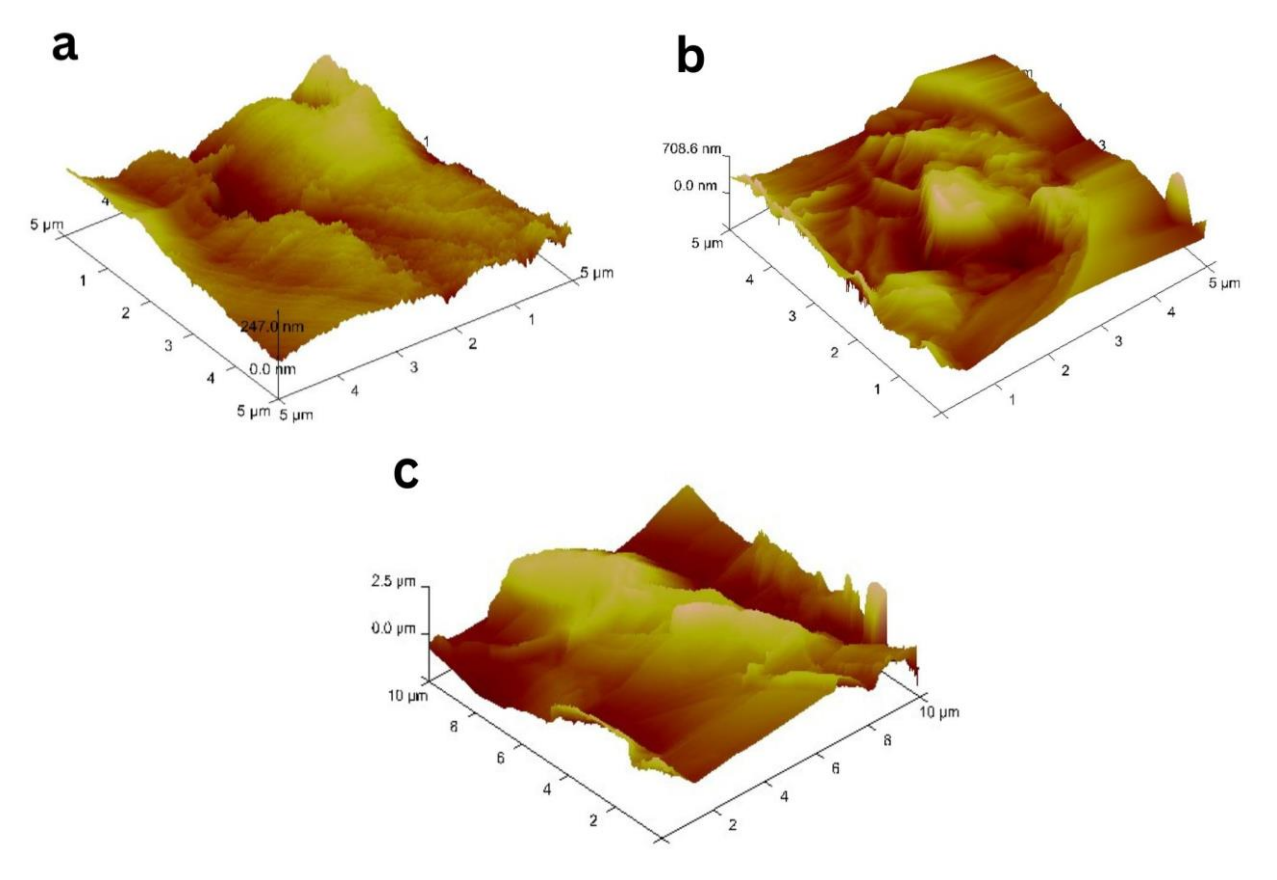


Figure 6. 3D view of the surface topography of the carbon paste modified with 8 wt.% np TiO<sub>2</sub> and (a) 40 vol.% PO) (scan size 5  $\mu$ m x 5  $\mu$ m, vertical scale 247 nm); (b) 40 vol.% TCP) (scan size 5  $\mu$ m x 5  $\mu$ m, vertical scale 708.6 nm), and (c) 40 vol.% POTCP (1:1) (scan size 10  $\mu$ m x 10  $\mu$ m, vertical scale 2.5  $\mu$ m)

The surface of the modified carbon paste electrode with the  $TiO_2$  nanoparticles and TCO binder has a layered structure. The graphite particles are characterized by sharp edges, relatively deep grooves (approx. 700 nm) and a layered structure (Figure 6b). The corresponding surface structures have a height of less than 1  $\mu$ m. The modified carbon paste with the  $TiO_2$  nanoparticles and the binder POTCP shows similar results to the carbon paste electrode modified with TCP. The graphite particles imaged with AFM (Figures 6b, 6c) show a similar structure to the particles imaged with SEM (Figures 1b, 1c).

The chemical characterization of the electrode material surface was performed using FTIR. FTIR spectra of the unmodified carbon paste (CPE, 40 vol.% PO, TCP, POTCP) and the modified carbon paste (MCPE) with TiO<sub>2</sub> nanoparticles (8 wt.% TiO<sub>2</sub>) are shown in Figure 7.

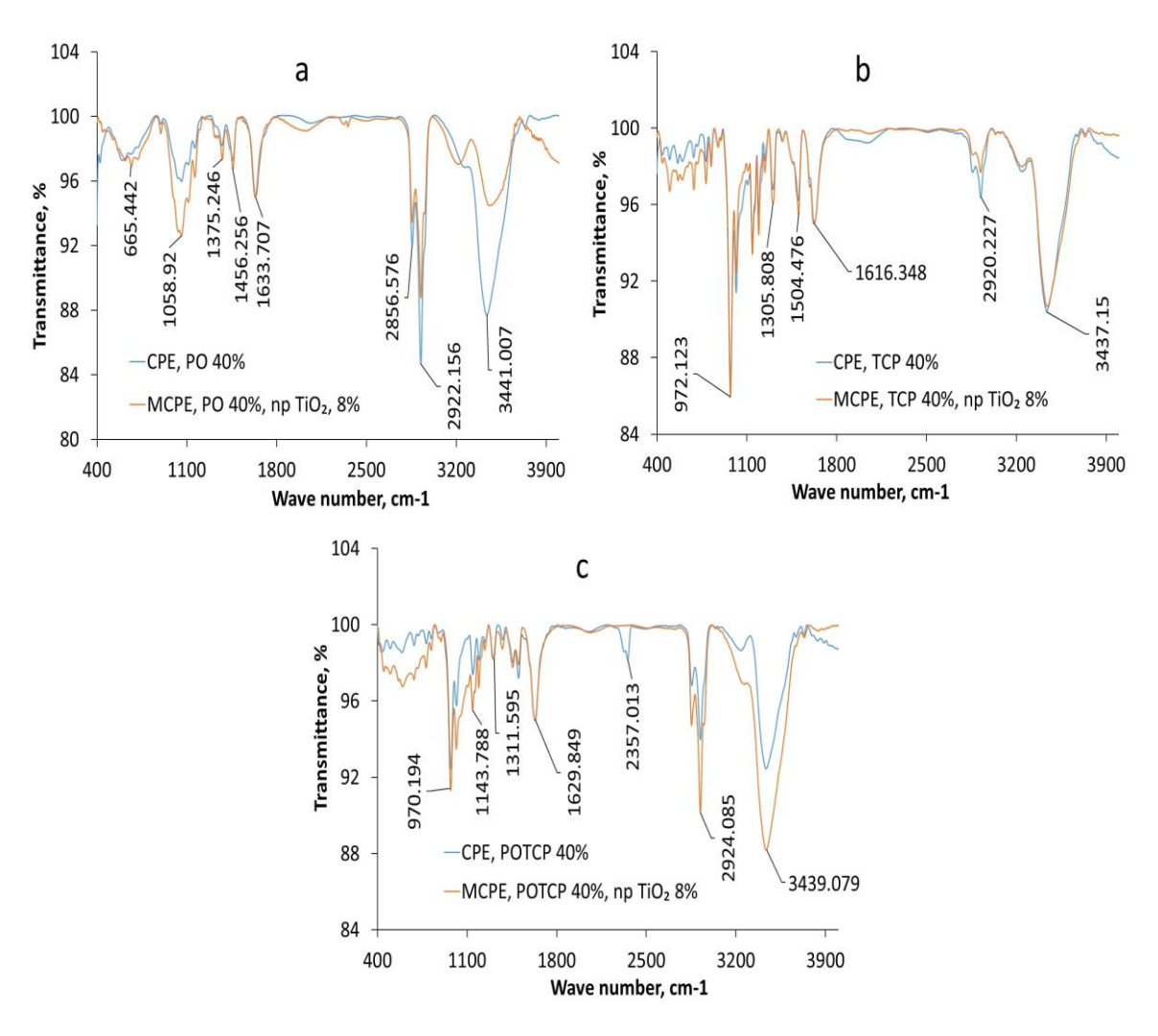


Figure 7. SEM images of the surfaces of unmodified (CPE) and modified carbon pastes (MCPE) with 8 wt.% np TiO<sub>2</sub> and 40 vol.% of (a) PO, (b) TCP and, (c) POTCP (1:1)

In the FTIR spectrum of the modified carbon paste with the TiO<sub>2</sub> nanoparticles and PO binder (Figure 7a), three characteristic C-H bands can be observed in the range of 2800–3000 cm<sup>-1</sup>. Two additional characteristic bands at 1375 and 1456 cm<sup>-1</sup> can also be attributed to C-H bonds [22]. Bands appearing above 3000 cm<sup>-1</sup> and around 1630 cm<sup>-1</sup> indicate the presence of water. The FTIR

spectrum of the modified carbon electrode with TCP (Figure 7b) clearly shows only the characteristic band sequence for TCP [23]. In the FTIR spectra of the carbon electrodes modified with TCP and POTCP, a broad peak in the range of 400–800 cm-¹ can also be observed, which can be attributed to Ti-O-Ti bending vibrations [24]. Furthermore, no additional peaks were detected in the FTIR spectra of the tested electrode materials, indicating that there are no chemical bonds between the individual components of the electrode material.

# Electrochemical characteristics of the modified carbon electrode

The electrochemical response of carbon electrodes modified with TiO<sub>2</sub> nanoparticles of the selected composition is shown in Figure 8.

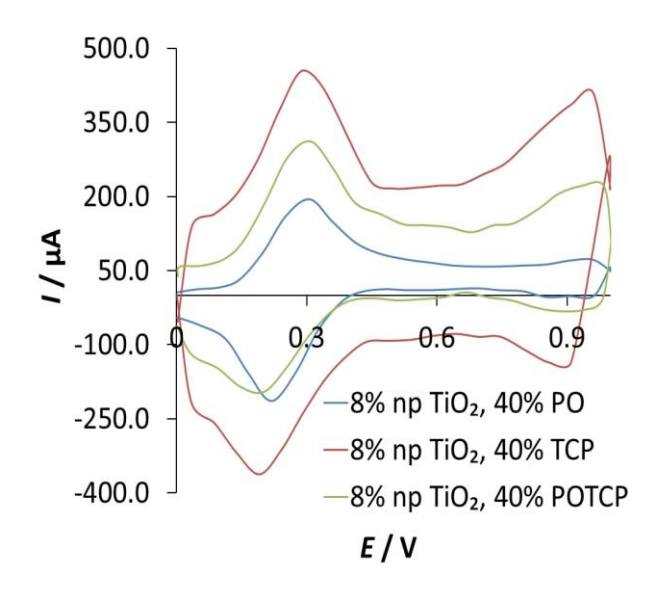


Figure 8. Cyclic voltammograms recorded on carbon paste electrode modified with 8 wt.%  $TiO_2$  np and 40 vol.% PO, TCP, and POTCP (1:1) in a 0.01 M  $K_4[Fe(CN)]_6 \times 3H_2O$  electrolyte

Cyclic voltammograms recorded with modified carbon electrodes with TiO<sub>2</sub> np and the binders PO, TCP and POTCP show clearly defined anodic current peaks. The highest anodic current intensity was observed for the electrode material with TCP, while the electrode with PO showed the lowest current intensity.

Based on the cyclic voltammograms, the electroactive surface area was determined using the Randles-Sevcik equation. The relative electroactive surfaces of the tested electrode materials with PO, POTCP and TCP are in a ratio of 1:1.6:2.3.

The tested binders showed no significant influence on the morphological characteristics of the surface of the electrode material, in contrast to the topographical characteristics. The analysis of the topographical characteristics as a function of the binder used shows a greater surface roughness for the electrode material with TCP (Ra = 130 nm) compared to the materials with PO (Ra = 38 nm) and POTCP (Ra = 116 nm). The increase or decrease in surface roughness may be caused by the presence of agglomerates formed during the preparation of the modified electrode paste or by the formation of nanoparticle agglomerates within the electrode material mass.

Araujo et al. have shown that the addition of a colloidal solution of Au nanoparticles to a carbon paste consisting of graphite powder and mineral oil leads to the formation of Au nanoparticle agglomerates [25].

On the other hand, the way in which the modified carbon paste is prepared influences the formation of agglomerates of different sizes. Melcher et al. have shown the dependence of the  $TiO_2$  agglomerate size on the preparation method and its duration [26].

It can be assumed that, in addition to the preparation method, adhesion forces between carbon, nanoparticles and binders also contribute to the formation of carbon and nanoparticle agglomerates of different sizes, which influence the surface roughness [27].

The surface of the electrode paste with PO has both the lowest roughness values and the least pronounced anodic current peak as well as the smallest electroactive surface area (0.13 cm²). The voltammograms show the most pronounced anodic current peak for the electrode paste with TCP, which is characterized by the largest electroactive surface area (0.30 cm²). For the electrode paste with POTCP, the electroactive surface area is 0.20 cm². The observed changes in the roughness values for the modified carbon pastes tested are therefore consistent with the results of cyclic voltammetry and the values of the electrochemically active surface area. Furthermore, these results are consistent with the lowest resistance and the highest degree of reversibility compared to the reversible standard redox system ([Fe(CN)]<sup>3-/4-</sup>) of the modified carbon electrodes tested [16].

In previous studies, AFM results showed an increase in roughness after the addition of Rudoped TiO<sub>2</sub> nanoparticles to the carbon paste (graphite powder and mineral oil in a ratio of 7:3), resulting in a larger electroactive surface area and a more intense anodic current response [28].

In addition, a pronounced presence of the capacitive current component can be observed in the cyclic voltammogram recorded with the modified carbon electrode with TCP, a pronounced presence of the capacitive current in this electrode composition can be attributed to the electrochemical activity of TCP [29]. TCP is easily subject to protonation with hydrogen ions according to the following equation:

$$(C_7H_7O)_3P=O+H^+ \rightarrow [(C_7H_7O)_3P=OH]^+$$
 (2)

Since TCP is embedded in the cathode material, it can be assumed that the reduction of the protonated form of TCP takes place and masks the signal resulting from the reduction of potassium ions [30]. Further investigation is required to clearly define the extent to which the effects of surface roughness and the capacitive current component influence the electrochemical response of the modified carbon electrode. The FTIR spectra indicate that no chemical bonds were formed between the individual components of the electrode material.

#### **Conclusions**

Based on the results presented, it is clear that the use of the tested binders primarily influences the topographical characteristics of the surface of the electrode material, which in turn influence the electrochemical properties of the electrode material. In addition to the method used to produce TiO<sub>2</sub> nanoparticles, the nature of binder also plays an important role in influencing the roughness of the electrode surface. These results underline the need to investigate the topographical characteristics when developing electrode materials from modified carbon paste.

#### **Conflicts of interest**

There are no conflicts of interest to declare.

#### References

- [1] J. Bai, B. Zhou, Titanium Dioxide Nanomaterials for Sensor Applications, *Chemical Reviews* **114** (2014) 10131–10176. <a href="https://doi.org/10.1021/cr400625j">https://doi.org/10.1021/cr400625j</a>
- [2] K. G. Manjunatha, B. E. Kumara Swamy, H. D. Madhuchandra, K. A. Vishnumurthy, Synthesis, characterization and electrochemical studies of titanium oxide nanoparticle modified carbon paste electrode for the determination of paracetamol in presence of adrenaline, *Chemical Data Collections* 31 (2021) 100604. https://doi.org/10.1016/j.cdc.2020.100604
- [3] J. Vatamanu, L. Cao, O. Borodin, D. Bedrov, G. D. Smith, On the Influence of Surface Topography on the Electric Double Layer Structure and Differential Capacitance of Graphite/Ionic Liquid Interfaces, *The Journal of Physical Chemistry Letters* **2** (2011) 2267-227. <a href="https://doi.org/10.1021/jz200879a">https://doi.org/10.1021/jz200879a</a>
- [4] D. Menshykau, I. Streeter, R. G. Compton, Influence of Electrode Roughness on Cyclic Voltammetry, *The Journal of Physical Chemistry C* **112** (2008) 14428–14438. https://pubs.acs.org/doi/10.1021/jp8047423
- [5] K. I. Popov, N. D. Nikolić, P. M. Živković, G. Branković, The effect of the electrode surface roughness at low level of coarseness on the polarization characteristics of electrochemical processes, *Electrochimica Acta* 55 (2010) 1919–1925. https://doi.org/10.1016/j.electacta.2009.10.085
- [6] N. P. Shetti, D. S. Nayak, Sh. J. Malode, R. M. Kulkarni, An electrochemical sensor for clozapine at ruthenium doped TiO<sub>2</sub> nanoparticles modified electrode, *Sensors and Actuators B: Chemical* **247** (2017) 858-867. <a href="https://doi.org/10.1016/j.snb.2017.03.102">https://doi.org/10.1016/j.snb.2017.03.102</a>.
- [7] D. S. Rajawat, N. Kumar, S. P. Satsangee, Trace determination of cadmium in water using anodic stripping voltammetry at a carbon paste electrode modified with coconut shell powder, *Journal of Analytical Science and Technology* **5** (2014) 19. <a href="http://www.jast-journal.com/content/5/1/19">http://www.jast-journal.com/content/5/1/19</a>
- [8] Y. Liu, X. Xu, C. Ma, F. Zhao, K. Chen, Morphology Effect of Bismuth Vanadate on Electrochemical Sensing for the Detection of Paracetamol, *Nanomaterials* **12** (2022) 1173. https://doi.org/10.3390/nano12071173
- [9] F. Sopaj, F. Loshaj, A. Contini, E. Mehmeti, A. Veseli, Preparation of an efficient and selective voltammetric sensor based on screen printed carbon ink electrode modified with TiO<sub>2</sub> nanoparticles for Azithromycin quantification, *Results in Chemistry* **6** (2023) 101123. <a href="https://doi.org/10.1016/j.rechem.2023.101123">https://doi.org/10.1016/j.rechem.2023.101123</a>
- [10] G. Dobrescu, R. Georgescu-State, F. Papa, J. F. v. Staden, R. N. State, Fractal Properties of Composite-Modified Carbon Paste Electrodes—A Comparison between SEM and CV Fractal Analysis, *Fractal and Fractional* 8 (2024) 205. <a href="https://doi.org/10.3390/fractalfract8040205">https://doi.org/10.3390/fractalfract8040205</a>
- [11] S. Oliveira Luciana, F. G. Alba Juan, L. Silva Valdinete, T. Ribeiro Rogério, H. L. Falcão Eduardo, M. Navarro, The effect of surface functional groups on the performance of Graphite powders used as electrodes, *Journal of Electroanalytical Chemistry*, **818** (2018) 106-113. <a href="https://doi.org/10.1016/j.jelechem.2018.04.022">https://doi.org/10.1016/j.jelechem.2018.04.022</a>
- [12] M. Khodari, G. A. M. Mersal, E. M. Rabie, H. F. Assaf, Electrochemical Sensor based on Carbon Paste Electrode Modified by TiO<sub>2</sub> nano-paricles for the Voltammetric Determination of Resorcinol, *International Journal of Electrochemical Science*, **13** (2018) 3460-3474. <a href="http://dx.doi.org/10.20964/2018.04.04">http://dx.doi.org/10.20964/2018.04.04</a>
- [13] S. I. Rabie Malha, A. A. Lahcen, F. Arduini, A. Ourari, A. Amine, Electrochemical Characterization of Carbon Solid\_like Paste Electrode Assembled Using Different Carbon Nanoparticles, *Electroanalysis* 27 (2015) 1-9. <a href="https://doi.org/10.1002/elan.201500637">https://doi.org/10.1002/elan.201500637</a>

- [14] G. S. Lobón, A. Yepez, L. F. Garcia, R. L. Morais, B. G. Vaz, V. V. Carvalho, G. A. Rodrigues de Oliveira, R. Luque, E. Gil, Efficient electrochemical remediation of microcystin-LR in tap water using designer TiO2@carbon electrodes, *Scientific Reports* **7** (2017) 41326. https://dx.doi.org/10.1038%2Fsrep41326
- [15] I. Švancara, A. Walcarius, K. Kalcher, K. Vytřas, Carbon paste electrodes in the new Millennium, *Central European Journal of Chemistry* **7** (2009) 598–656. https://doi.org/10.2478/s11532-009-0097-9
- [16] S. Mićin, B.N. Malinović, T. Đurčić, Development and characterization of electrochemical sensors based on carbon modified with TiO<sub>2</sub> nanoparticles, *Hemijska Industrija* **76** (2022) 147-158. <a href="https://doi.org/10.2298/HEMIND220105013M">https://doi.org/10.2298/HEMIND220105013M</a>
- [17] S. Mićin, N. Ivošević DeNardis, S. Martinez, V. Špada, B. N. Malinović, Characterization of wine polyphenols with a carbon/nanoparticle TiO<sub>2</sub> electrode, *Journal of Electrochemical Science and Engineering* **14** (2024) 583–599. https://doi.org/10.5599/jese.2395
- [18] X. Jiang, M. Manawan, T. Feng, R. Qian, T. Zhao, G. Zhou, F. Kong, Q. Wang, S. Dai, J. H. Pan, Anatase and rutil in evonik aeroxide P25: Heterojunctioned or individual nanoparticles, *Catalysis Today* **300** (2017) 12-17. http://dx.doi.org/10.1016/j.cattod.2017.06.010
- [19] M.H. Mashhadizadeh, E. Afshar, Electrochemical investigation of clozapine at TiO<sub>2</sub> nanoparticles modified carbon paste electrode and simultaneous adsorptive voltammetric determination of two antipsychotic drugs, *Electrochimica Acta* **87** (2013) 816-823. <a href="https://doi.org/10.1016/j.electacta.2012.09.004493">https://doi.org/10.1016/j.electacta.2012.09.004493</a>
- [20] I. Piljac, *Senzori fizikalnih veličina i elektroanalitičke metode*, Media print, Zagreb, Hrvatska, 2010. ISBN 978-953-58487-0-7
- [21] T. Radoman, J. Džunuzović, K. Jeremić, A. Marinković, P. Spasojević, I. Popović, E. Džunuzović, Uticaj veličine nanočestica TiO<sub>2</sub> i njihove površinske modifikacije na reološka svojstva alkidne smole, *Hemijska Industrija* **67** (2013) 923-932. https://doi.org/10.2298/HEMIND131106081R
- [22] R. A. Farghali, R. A. Ahmed, A. A. Alharthi, Synthesis and Characterization of Electrochemical Sensor Based on Polymeric/TiO<sub>2</sub> Nanocomposite Modified with Imidizolium Ionic Liquid for Determination of Diclofenac, *International Journal of Electrochemical Science* **13** (2018) 10390 10414. https://doi.org/10.20964/2018.11.16
- [23] National Center for Biotechnology Information, https://pubchem.ncbi.nlm.nih.gov/compound/6529#section=FTIR-Spectra (accessed 11. 05. 2024).
- [24] S. K. Sivan, S. Sh. Shankar, N. Sajina, A. K. Padinjareveetil, R. Pilankatta, V. B. Sameer Kumar, B. Mathew, B. George, P. Makvandi, M. Černík, V. V. T. Padil, R. S. Varma, Fabrication of a Greener TiO2@Gum Arabic-Carbon Paste Electrode for the Electrochemical Detection of Pb2+ Ions in Plastic Toys, ACS Omega 5 (2020) 25390–25399. https://pubs.acs.org/doi/full/10.1021/acsomega.0c03781
- [25] V. M. Araujo, O.A. Pinto, V. I. Paz Zanini, Addressing the surface coverage of Au nanoagglomerates and the electrochemical properties of modified carbon paste electrodes: Experimental and theoretical studies on ascorbic acid oxidation, *Colloids and Surfaces B: Biointerfaces* **200** (2021) 111585. https://doi.org/10.1016/j.colsurfb.2021.111585
- [26] J. Melcher, N. Barth, C. Schilde, A. Kwade, D. Bahnemann, Influence of TiO<sub>2</sub> agglomerate and aggregate sizes on photocatalytic activity, *Journal of Materials Science* **52** (2016) 1047–1056. <a href="https://doi.org/10.1007/s10853-016-0400-z">https://doi.org/10.1007/s10853-016-0400-z</a>
- [27] F. Pellegrino, L. Pellutiè, F. Sordello, C. Minero, E. Ortel, V-D. Hodoroaba, V. Maurino, Influence of agglomeration and aggregation on the photocatalytic activity of TiO<sub>2</sub> nanoparticles, *Applied Catalysis B: Environmental* **216** (2017) 80-87. <a href="https://doi.org/10.1016/j.apcatb.2017.05.046">https://doi.org/10.1016/j.apcatb.2017.05.046</a>



- [28] N. P. Shettia, D. S. Nayaka, S. J. Malodea, R. M. Kulkarni, An electrochemical sensor for clozapine at ruthenium doped TiO<sub>2</sub> nanoparticles modified electrode, *Sensors and Actuators B* **247** (2017) 858–867. <a href="http://dx.doi.org/10.1016/j.snb.2017.03.102">http://dx.doi.org/10.1016/j.snb.2017.03.102</a>
- [29] I. Švancara, J. Konvalina, K. Schachl, K. Kalcher, K. Vytras, Stripping voltammetric determination of iodide with synergistic accumulation at a carbon paste electrode, Electroanalysis 10 (1998) 435-441. <a href="https://doi.org/10.1002/(SICI)1521-4109(199805)10:6<435::AID-ELAN435>3.0.CO;2-J">https://doi.org/10.1002/(SICI)1521-4109(199805)10:6<435::AID-ELAN435>3.0.CO;2-J</a>
- [30] J. Đorđević, Z. Papp, V. Guzsvány, I. Švancara, T.Trtić-Petrović, M. Purenović, K. Vytřas, Voltammetric Determination of the Herbicide Linuron Using a Tricresyl Phosphate-Based Carbon Paste Electrode, *Sensors* **12** (2012) 148-161. <a href="https://doi.org/10.3390/s120100148">https://doi.org/10.3390/s120100148</a>

© 20xx by the authors; licensee IAPChem, Zagreb, Croatia. This article is an open-access article distributed under the terms and conditions of the Creative Commons Attribution license (http://creativecommons.org/licenses/by/4.0/) (cc) EY